The United Nations University

GEOTHERMAL TRAINING PROGRAMME
Orkustofnun, Grensásvegur 9,
IS-108 Reykjavík, Iceland

Reports 2006
Number 15

HYDROGEN SULPHIDE DISPERSION AND MODELLING FOR NESJAVELLIR POWER STATION USING GAUSSIAN AND NUMERICAL MODELS

E. Munene Nyagah
Kenyatta University, Department of Physics
P.O Box 43844-00100
Nairobi
KENYA
nyagahevans@yahoo.com

ABSTRACT

The spatial variation of hydrogen sulphide fallout around Nesjavellir geothermal power station has been determined using Gaussian (AERMOD) and numerical models. The models quantitatively simulated atmospheric interactions and related the emission of hydrogen sulphide to air quality. The simulations, based on data from June to August 2006, were aimed at quantifying the distribution of hydrogen sulphide within the vicinity of the power station as well as validating the numerical model. The predicted concentrations were lower than the field measurements collected within the modelling area. The near-ground predictions from the two models demonstrate that hydrogen sulphide emitted from the power station undergoes significant dilution as it is dispersed by wind, resulting in low concentrations in the neighbourhood of the power station, albeit with localised high concentrations to the immediate east of the power station. The study indicates that the models can capture the real-time features governing the dispersal of hydrogen sulphide. Despite some inaccuracies, the numerical model predictions represent well the actual dispersion and with some modifications they can be adopted for use in quantifying the dispersion of gaseous emissions elsewhere.

1. INTRODUCTION

Geothermal energy is a leading source of renewable energy for power generation and the provision of hot water. It is an environmentally friendly energy source, especially when compared to fossil-fuel sources (Noorollahi and Yousefi, 2003). However, all geothermal development has some impact on the environment (Gunnlaugsson, 2003). These impacts vary during the various developmental phases. For instance, it is minimal during the early exploration phase prior to drilling, but when drilling commences there are often more serious impacts on the physical environment. The main effects are related to surface disturbances, physical effects due to fluid withdrawal, noise, thermal effects and discharge of non-condensable gases, and the release of fine solid particles into the atmosphere (Kristmannsdóttir and Ármannsson, 2003). The main geothermal gases are carbon dioxide and hydrogen sulphide. Other gases, in trace quantities, include hydrogen, methane, nitrogen, radon and oxygen.

1.1 Background and rationale

Hydrogen sulphide emissions are a natural consequence of geothermal exploitation. The most important points of emission in plants are chimneys for venting the non-condensable gases. Others are evaporation at cooling towers, silencers, drainage and traps in the vapour-ducts (steam pipes) and elimination of excess condensate from the cooling towers. The gas is toxic in high concentrations and has a very unpleasant smell in low concentrations (Kristmannsdóttir et al., 1997). Public health scientists now recognise that hydrogen sulphide is a potent neuro-toxin and exposure to low ambient levels causes irreversible damage to the brain and central nervous system (Hayward, 2001). The sense of smell for hydrogen sulphide is lost at a concentration below that at which it is harmful, so people may have little warning of the presence of the gas at dangerous concentrations (Hirsch and Zavala, 1999).

The presence of hydrogen sulphide in the atmosphere induces corrosion of aluminium and copper conductors in sub-stations and on transmission lines. Exciter commutators of copper can be very troublesome, because not only is the copper itself attacked by hydrogen sulphide but the sulphide film also causes sparking at the brushes, causing erosion (Sinclair Knight et. al., 1994). With increased emphasis on the environmental viability of energy projects, these effects need to be identified, quantified and, if necessary, eliminated or abated. To reduce environmental impacts, monitoring and control measures must be put in place. To achieve this, the extent of contamination must be ascertained quickly and in near-real-time. One way to undertake this is to make use of models which can predict the spatial distribution and concentration of the pollutant with time.

Mathematical models are used in all aspects of air quality planning and monitoring where prediction is a major component, from episodic forecasting to long-term monitoring. In general, Gaussian and numerical models are widely used for the simulation of air quality. The models simulate the atmosphere in varying degrees of detail by mathematically representing emissions, with initial and boundary concentrations of chemical species (Tonnesen et al., 1998). In this way, an understanding of the atmosphere's chemistry and meteorology is combined with estimates of source emissions to predict possible ground-level concentrations. This timely and reliable information gained from air quality forecasts forms a basis for developing and making managerial decisions about environmental damage. Additionally, forecasts provide information on real-time emission abatement strategies, facilitating the protection of the public from the impacts of air pollution.

1.2 Aims and objectives

The goal of this project is to simulate the dispersion of hydrogen sulphide emitted from Nesjavellir power station in Iceland using Gaussian and numerical models. The simulated results will be compared with field measurements taken at some receptor locations within the geothermal field in June 2006. A comparison of the prediction performance of the two models will be made with a view of validating the numerical model. The validation will shed light on whether the model can be used to quantify the dispersion of gaseous pollutants elsewhere after comparing its performance against that of a well rated model (ISC AERMOD View) (Brode, 2006). Presently, there are very few Kenyan scientists working in this area. This results in the hiring of overseas scientists and models to simulate air quality for both developed and non-developed geothermal fields. This is in line with the requirement of the World Bank that a comprehensive environmental audit be carried out whenever a new power-plant is being built or an existing facility undergoes significant modification (World Bank, 1998). The bank is the main financier of geothermal projects in Kenya and other developing countries.

2. NESJAVELLIR GEOTHERMAL AREA

2.1 Overview

Nesjavellir geothermal co-generation (electricity and hot water) power plant is located within Nesjavellir geothermal field, a high-enthalpy geothermal system sited within the Hengill central volcano in SW-Iceland (Figure 1). Geothermal investigations at Nesjavellir commenced in 1946. However, it was not until 1986 that a decision was made to harness the geothermal heat for district heating in Reykjavík (Gunnarsson et al., 1992). Nesjavellir power plant was commissioned in 1990 with a capacity to generate 100 MW thermal by producing about 560 l/s of hot water at 82°C for district heating. In 1995, the capacity was expanded to 150 MW thermal and in 1998 to 200 MW thermal and the production of 60 MW electricity commenced. Reykjavik Energy is currently operating 120 MW electric (MWe) and 300 MW thermal (MWt) power-plant units in the Nesjavellir field.

In the Nesjavellir power plant, all spent geothermal fluid is discharged into the environment. The geothermal fluids from the wells are piped to the separating station and separated into liquid and steam that go directly to turbines and heat exchangers. The non-condensable gases are pumped to the cooling tower and released at a high-upward velocity below the cooling tower fans. The gases mix with the rising hot plume. The mixture is then blown out vertically to the atmosphere by the cooling tower fans where dispersion and cooling occurs.

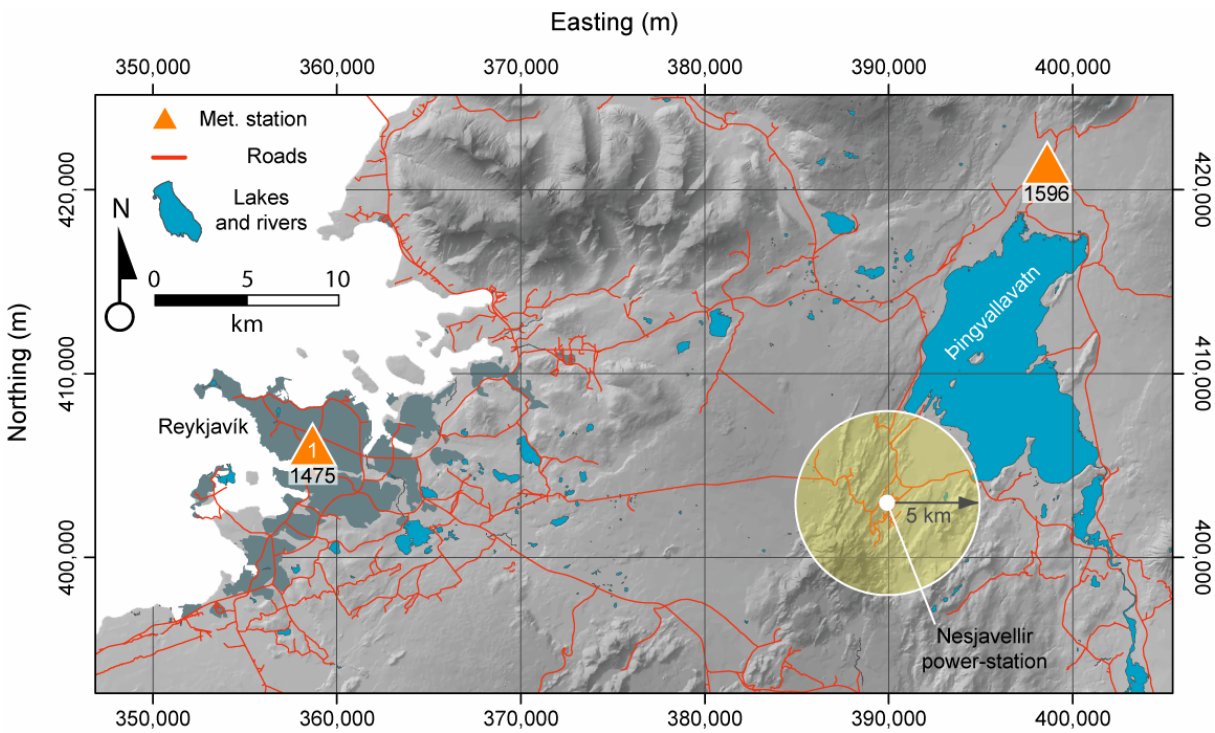

FIGURE 1: Map of the Reykjavik area showing Nesjavellir geothermal area, power station, meteorological stations and the surrounding areas; the map projection is Lambert Conformal Conic and data are referenced to the ISN93 datum. The circle around the site of the power station defines the extent of the study area

2.2 Environmental impacts of utilization

The main environmental effects associated with the utilization of Nesjavellir geothermal area are related to the discharge of waste water and the release of non-condensable gases into the environment.

The main non-condensable gases in the steam are carbon dioxide and hydrogen sulphide. Presently, 13,259 tons of carbon dioxide and 8,918 tons of hydrogen sulphide are discharged from the plant annually (Gissurarson and Sigurjónsson, 2006). Other pollutants include silica, boron, arsenic and aluminium.

Nesjavellir geothermal field has both high production and high hydrogen sulphide concentrations in the steam and contributes the most hydrogen sulphide emissions in Iceland (Kristmannsdóttir et al., 1997). Although Nesjavellir geothermal field, like other geothermal fields in Iceland, is in a sparsely populated area, the environmental sensitivity of the area is high due to its proximity to Lake Thingvallavatn, which is fringed by summer houses and is a popular tourist attraction (Figure 1). This, however, does not place it in the same league with some other geothermal areas in the world which lie in very sensitive areas. Olkaria geothermal field in Kenya, for example, lies in the middle of a game park and close to highly productive flower farms whose economic activities have attracted a large human population (Marani et al., 1995). Miravalles geothermal field in Costa Rica, on the other hand, lies within the towns Guayabo and La Fortuna (Guido, 1999), requiring close monitoring and controls of hydrogen sulphide emissions into the atmosphere. The understanding of how the gas disperses and the level of contamination on the immediate and distant areas is of importance, especially in areas where the resource is located in or close to environmentally sensitive areas.

2.3 Monitoring the dispersion of hydrogen sulphide

Monitoring of hydrogen sulphide concentrations in the Nesjavellir geothermal field dates back to 1992. Short-term measurements of hydrogen sulphide concentrations were aimed at obtaining the range and reference values for further monitoring. Locations were based on the results of point measurements of hydrogen sulphide in a grid over the area of visible activity (Kristmannsdóttir et al., 2000). The measurements were both point measurements and measurements based on sampling of gases over 24 hours in wetted filters and liquids. The hydrogen sulphide concentration was found to range between 1 and 200 $\mu g/m^3$.

Long-term measurements, extending over four to six months, were started in 1995. Two monitoring stations, which also hosted weather observation sites, were operated for one year. The project was officially terminated at the end of 1997. According to Gíslason (2000), monitoring in Nesjavellir is a continuous process as samples of geothermal water and steam are collected monthly for analysis of non-condensable gases. Although measurements comprise an important aspect of monitoring, alone they are rarely sufficient for giving the desired best possible description of the time and space variation of either deposition or concentrations (Moussiopoulos et al., 1997). Dispersion models provide timely and reliable information on the state of the environment, being a basis for developing and making managerial decisions in the field of nature protection by the environmental management bodies and other agencies.

As an alternative to, or in conjunction with, direct monitoring, computer models are often used to predict the levels of pollutants emitted from various types of sources, and how these emissions eventually impact ambient air quality over time. As a monitoring tool, modelling is generally a cost-effective replacement for direct field measurement of ambient air quality. Models give information at many locations, can simulate future scenarios and can be performed regularly. They are designed to quantitatively simulate the atmospheric interactions and relate the emission of pollutants to the air-quality. The underlying assumption is that given a high degree of understanding of the processes by which stresses on a system produce subsequent responses in that system, the system's response to any set of stresses can be predetermined, even if the magnitude of the new stresses falls outside of the range of historically observed stresses.

Simulation studies focussing on the dispersal of gaseous pollutants in Nesjavellir geothermal field have been carried out before. Noorollahi (1999) used a Gaussian model (ISC3view) to simulate the

dispersion of both hydrogen sulphide and carbon dioxide. The results from the model show that the hydrogen sulphide concentrations were lower than those specified in workplace standards. Since then, two additional turbines have been installed and hydrogen sulphide release increased from 3,700 in 1999 to 8,700 tons per year. In addition, one of the dispersion models (ISC AERMOD View) being used in this study is an improvement of the model used previously. Consequently, hydrogen sulphide distribution simulation should be carried out to ascertain whether the near-ground concentrations are below the specified workplace standards.

3. MODEL DESCRIPTIONS

3.1 ISC-AERMOD View

AERMOD is a Gaussian model that was developed by AMS (American Meteorological Society) in collaboration with EPA (Environmental Protection Agency) as a replacement for an earlier ISC3 View model. The description given below is based on Cimorelli et al. (2004). The model can be applied to rural and urban areas, flat and complex terrain, surface and elevated releases, and multiple sources (including, point, area and volume sources). In the stable boundary layer (SBL), it assumes the concentration distribution to be Gaussian in both the vertical and horizontal plane. In the convective boundary layer (CBL), the horizontal distribution is also assumed to be Gaussian, but the vertical distribution is described with a bi-Gaussian probability density function.

AERMOD characterizes the planetary boundary layer (PBL) through both surface and mixed layer scaling. Through a meteorological pre-processor AERMET, the model constructs vertical profiles of required meteorological variables based on measurements and extrapolations of those measurements using similarity (scaling) relationships. AERMET passes the information to AERMOD.

3.1.1 The diffusion equation

For a steady-state Gaussian plume, the hourly concentration at downwind distance x (m) and crosswind distance y (m) is given by:

$$X = \frac{QKVD}{2\pi\mu_s\sigma_y\sigma_z}\exp\left[-0.5\left(\frac{Y}{\sigma_y}\right)^2\right] \tag{1}$$

where Q is the pollutant emission rate (mass per unit time); K is the scaling unit to convert the calculated calculations to desired units (default value for Q is 1×10^6 g/s and the concentration is in μg/m^3); V is the vertical term; D is the decay term; σ_y, σ_x are the standard deviations of lateral and vertical concentration distribution (m); and μ_s is the wind speed at release height (m/s).

3.1.2 Source parameters

The input to the model includes the location, elevation, emission rate, stack height, stack gas temperature, stack gas exit velocity, and stack inside diameter. Other parameters include the dimensions of the buildings and stack(s) and their references relative to the modelling field.

3.1.3 Meteorological pre-processor (AERMET)

The purpose of AERMET is to use meteorological measurements, representative of the modelling domain, to compute certain boundary layer parameters used to estimate profiles of wind, turbulence and temperature. A brief description of the basic formulation of AERMET is given below. In the

convective boundary layer, AERMET computes the surface friction velocity u_* and the Monin-Obukhov length, L. The expression for u_* (e.g., Panofsky and Dutton, 1984) is:

$$u_* = \frac{ku_{ref}}{\ln(z_{ref}/z_0) - \psi_m\{z_{ref}/L\} + \psi_m\{z_0/L\}} \tag{2}$$

where k is the von Karman constant (=0.4); u_{ref} is the wind speed at reference height; z_{ref} is the reference measurement height for wind in the surface layer; z_0 is the roughness length; and ψ_m is the stability term.

The stability terms are calculated as follows:

$$\psi_m\{z_{ref}/L\} = 2\ln(^{1+\mu}/_2) + \ln(^{1+\mu^2}/_2) - 2\tan^{-1}\mu + {}^{\pi}/_2 \tag{3a}$$

$$\psi_m\{z_0/L\} = 2\ln(^{1+\mu_0}/_2) + \ln(^{1+\mu_0^2}/_2) - 2\tan^{-1}\mu_0 + {}^{\pi}/_2 \tag{3b}$$

where $\mu = (1 - 16z_{ref}/z_0)^{1/4}$ and $\mu_0 = (1 - 16z_0/L)^{1/4}$

Assuming that $\psi_m = 0$ (neutral limit) and setting u = u_{ref}, L is calculated from the following definition (Wyngaard, 1988):

$$L = -\frac{\rho C_p T_{ref} u_*^3}{kgH} \tag{4}$$

where g is the acceleration of gravity; C_p is the specific heat of air at constant pressure; ρ is the density of air, H is the sensitive heat flux; and T_{ref} is the ambient temperature representative of the surface layer.

Convective velocity scale w^* is used to characterize the convective portion of the turbulence in the CBL. Thus, in order to estimate turbulence, an estimate of w^* is needed. AERMET calculates the convective velocity scale from its definition (Wyngaard, 1988) as:

$$w^* = \left(\frac{gHz_{ic}}{\rho C_p T_{ref}}\right)^{1/3} \tag{5}$$

where z_{ic} is the convective mixing height.

In the stable boundary layer, the energy budget term associated with the ground heating component is highly site-specific. During the day, this component is only about 10% of the total net radiation, while at night, its value is comparable to that of the net radiation (Oke, 1978). Therefore, errors in the ground heating term can generally be tolerated during the daytime, but not at night. To avoid using a nocturnal energy balance approach that relies upon an accurate estimate of ground heating, AERMIC has adopted a much simpler semi-empirical approach for computing u_* and L. The computation of u_* depends on the empirical observation that the temperature scale, θ_*, defined as:

$$\theta_* = -H / \rho C_p u_* \tag{6}$$

varies little during the night.

Following the logic of Venkatram (1980), the definition of L in Equation 4 is combined with Equation 6 to express the Monin-Obukhov length in the SBL as:

$$L = \frac{T_{ref}}{kg\theta_*} u_*^2 \tag{7}$$

From (Panofsky and Dutton, 1984) the wind-speed profile in stable conditions takes the form:

$$u = \frac{u_*}{k}\left[\ln\left(\frac{z}{z_0}\right) + \frac{\beta_m z_{ref}}{L}\right] \tag{8}$$

where $\beta_m = 5$ and z_{ref} is the wind speed reference measurement height.

Substituting Equation 7 into Equation 8 and defining the drag coefficient, C_D as k / ln(z_{ref}/z_0) (Garratt, 1992), results in:

$$\frac{u}{u_*} = \frac{1}{C_D} + \frac{\beta_m z_{ref} g\theta_*}{T_{ref} u_*} \tag{9}$$

Multiplying Equation 8 by $C_D\, u_*^2$ and rearranging yields a quadratic of the form:

$$u_*^2 - C_D u u_* + C_D u_0^2 = 0 \tag{10}$$

where $u_0^2 = \beta_m z_{ref} g\theta_* / T_{ref}$

The quadratic equation has the following solution:

$$u_* = \frac{C_D u_{ref}}{2}\left[-1 + \left(1 + \left(\frac{2u_0}{C_D^{1/2} u_{ref}}\right)^2\right)^{1/2}\right] \tag{11}$$

Equation 11 produces real-valued solutions only for when the wind speed is greater than or equal to the critical value, $u_{cr} = \left[4\beta_m z_{ref} g\theta / T_{ref} C_D\right]^{1/2}$.

For wind speeds less than the critical value, u_* and θ_* are parameterized using the following linear expression:

$$\begin{aligned} u_* &= u_*\{u = u_{cr}\}(u / u_{cr}) && \text{for } u < u_{cr} \\ \theta_* &= \theta_*(u / u_{cr}) && \text{for } u < u_{cr} \end{aligned} \tag{12}$$

In order to calculate u_* from Equation 11 an estimate of θ_* is needed. If representative cloud cover observations are available the temperature scale in the SBL is taken from the empirical form of Van Ulden and Holtslag (1985) as:

$$\theta_* = 0.09(1 - 0.5n^2) \tag{13}$$

where n = The fractional cloud cover.

However, if cloud cover measurements are not available, an estimate of θ_* is made from measurements of temperature at two levels and wind speed at one level. This technique, known as the Bulk Richardson approach, starts with the similarity expression for potential temperature (Panofsky and Dutton, 1984), that is:

$$\theta\{z\} - \theta_0 = \frac{\theta_*}{k}\left(\ln\frac{z}{z_0} + \beta_m \frac{(z_2 - z_1)}{L}\right) \tag{14}$$

where β_m = 5 and k = 0.4 is the von Karman constant. Applying Equation 14 to the two levels of temperature measurements and re-arranging terms yields:

$$\theta_* = \frac{k(\theta_2 - \theta_1)}{\left[\left(\ln\frac{z_2}{z_1}\right) + \beta_m \frac{(z_2 - z_1)}{L}\right]} \tag{15}$$

For situations in which $z / L \leq 5$, u_* is estimated using Equation 8, (for more stable cases), u_* is calculated as follows:

$$u_* = \frac{ku}{\left[\ln\frac{z}{z_0} + 7\ln\frac{z}{L} + \frac{4.25}{z/L} - \frac{0.5}{(z/L)^2} + \frac{\beta_m}{2} - 1.648\right]} \tag{16}$$

3.1.4 Wind speed profiling

The profile equation for wind speed has a logarithmic form (Cimorelli et al., 2004):

$$u = u\{7z_0\}\left[\frac{z}{7z_0}\right] \qquad \text{for } z < 7z_0 \tag{17a}$$

$$u = \frac{u_*}{k}\left[\ln\left(\frac{z}{z_0}\right) - \psi_m\left\{\frac{z}{L}\right\} + \psi_m\left\{\frac{z_0}{L}\right\}\right] \qquad \text{for } 7z_0 \leq z \leq z_i \tag{17b}$$

$$u = u\{z_i\} \qquad \text{for } z > z_i$$

At least one wind speed measurement that is representative of the surface layer is required for each simulation. Since the logarithmic form does not adequately describe the profile below the height of obstacles or vegetation, the above equation allows for a linear decrease in wind speed from its value at $7z_0$.

For both the CBL and SBL, wind direction is assumed to be constant with a height that is both above the highest and below the lowest measurements.

3.1.5 Turbulence

The total vertical velocity variance or turbulence in the CBL is given as:

$$\sigma_{wT}^2 = \sigma_{wc}^2 + \sigma_{wm}^2$$

where σ_{wc} and σ_{wm} are the convective and mechanical portions of the vertical turbulence, respectively.

The convective portion is calculated as:

$$\sigma_{wc}^2 = 1.6\left(\frac{z}{z_{ic}}\right).w_*^2 \qquad \text{for } z \le 0.1\ z_{ic} \qquad (18a)$$

$$\sigma_{wc}^2 = 0.35 w_*^2 \qquad \text{for } 0.1\ z_{ic} \le z \le z_{ic} \qquad (18b)$$

$$\sigma_{wc}^2 = 0.35 w_*^2 \exp\left[-\frac{6(z - z_{ic})}{z_{ic}}\right] \qquad \text{for } z > z_{ic} \qquad (18c)$$

where w_* is a strongly convective limit and he expression for $z \le 0.1\ z_{ic}$ is the free convection limit (Panofsky et al., 1977), the expression for $0.1\ z_{ic} \le z \le z_{ic}$ is the mixed-layer value (Hicks,1985), and for $z > z_{ic}$ is a parameterization to connect the mixed layer σ^2_{wc} to the assumed near-zero value well above the CBL.

The mechanical turbulence is assumed to consist of a contribution from the boundary layer σ_{wml} and from a "residual layer" σ_{wmr} above the boundary layer $z > z_i$ such that:

$$\sigma_{wm}^2 = \sigma_{wml}^2 + \sigma_{wmr}^2$$

The expression for σ_{wml} following the form of Brost et al., (1982) is:

$$\sigma_{wml} = 1.3 u_*\left(1 - \frac{z}{z_i}\right)^{1/2} \qquad \text{for } z < z_i \qquad (19a)$$

$$\sigma_{wml} = 0.0 \qquad \text{for } z \ge z_i \qquad (19b)$$

Above the mixing height σ_{wmr} is set equal to the average of measured values in the residual layer above z_i. If measurements are not available, then σ_{wmr} is taken as the default value of 0.02 $u\{z_i\}$. The constant 0.02 is the assumed turbulence intensity i_z (= σ_{wm} / u), for the very stable conditions presumed to exist above z_i (Briggs, 1973). Within the mixed layer, the residual turbulence (σ_{wmr}) is reduced linearly from its value at z_i to zero at the surface.

In the SBL the vertical turbulence contains only a mechanical portion which is given by Equation 19. The use of the same σ_{wm} expressions for the SBL and CBL is done to ensure continuity of turbulence in the limit of neutral stability.

In the CBL the total lateral turbulence, σ^2_{vT}, is computed as a combination of a mechanical σ_{vm} and convective σ_{vc} portion such that:

$$\sigma_{vT}^2 = \sigma_{vc}^2 + \sigma_{vm}^2$$

In the SBL the total lateral turbulence contains only a mechanical portion. AERMOD uses the same σ_{vm} expression in the CBL and SBL. A description of mechanical and convective profiles of lateral turbulence follows. Between the surface and the top of the mechanically mixed layer, σ^2_{vm} is assumed to vary linearly as:

$$\sigma_{vm}^2 = \left[\frac{\sigma_{vm}^2\{z_{im}\} - \sigma_{v0}^2}{z_{im}}\right] z + \sigma_{vo}^2 \qquad \text{for } z \le z_{im} \qquad (20a)$$

$$\sigma_{vm}^2 = \sigma_{vm}^2\{z_{im}\} \qquad \text{for } z > z_{im} \qquad (20b)$$

where σ_{vo} is the surface value of the lateral turbulence.

Above the mixed layer, AERMOD adopts a typical value of 0.5 ms^{-1} for σ_{vc}, the residual lateral turbulence. The convective portion of the lateral turbulence within the mixed layer is calculated as:

$$\sigma_{vc}^2 = 0.35 w_*^2$$

3.1.6 Plume rise calculations

In the CBL, the plume rise Δh_s for the direct source is given by the superposition of source momentum and buoyancy effects following Briggs (1984):

$$\Delta h_d = \left(\frac{3F_m x}{\beta_1^2 u_p^2} + \frac{3}{2\beta_1^2} \cdot \frac{F_b x^2}{u_p^3} \right)^{1/3} \tag{21}$$

where F_m is the stack momentum flux, F_b is the stack buoyant flux, β_1 is an entrainment parameter and u_p is the wind speed used for calculating plume rise.

In the SBL, the plume rise is taken from Wiel (1988) as:

$$\Delta h_s = 2.66 \left(\frac{F_b}{N^2 u_p} \right)^{1/3} \cdot \left[\frac{N' F_m}{F_b} \sin\left(\frac{N' x}{u_p} \right) + 1 - \cos\left(\frac{N' x}{u_p} \right) \right]^{1/3} \tag{22}$$

where N′ = 0.7 N and N is the Brunt-Vaisala frequency.

3.1.7 Summary

AERMOD, with some few exceptions, serves as a complete replacement for ISC3. It contains new or improved algorithms for: dispersion in the convective and stable boundary layers, plume rise and buoyancy, plume penetration into elevated inversions, computation of vertical profiles of wind, turbulence, and temperature, and the treatment of building wake effects among others. It has a meteorological pre-processor AERMET which uses meteorological data and surface characteristics to calculate boundary layer parameters (e.g., mixing height, friction velocity, etc.). This data, whether measured off-site or on-site, must be representative of the meteorology in the modelling domain.

3.2 The numerical model

The numerical model is a Eurelian model developed by the author as part of an MSc thesis written between 2003 and 2005 (Nyagah et al., 2006). It is a three dimensional eulerian model with non-terrain-following mesh using the integral finite difference discretisation. It includes modules for transport (advection and diffusion), dry deposition, wet deposition and chemical transformation. The model can be used to determine the dispersion of any gas, both reactive and non-reactive. It can accommodate both continuous discharge and single puffs resulting from spillage accidents. The source parameters include stack dimensions, amount of pollutant emitted, temperature and velocity at which the pollutant is emitted. Wind speed and direction, temperature, radiation and rainfall are the meteorological parameters. The sink (decay) parameters include depositions both wet and dry as well as chemical transformation.

3.2.1 The dispersion equation

The concentrations of hydrogen sulphide, $C(\vec{r}, t)$ at time t and place $\vec{r} = x, y, z,$ are calculated by numerically solving the transport-transformation equation (Cemas and Rakovec, 2003):

$$\frac{\partial C}{\partial t} + \overline{v} \cdot \nabla C = \nabla(K \nabla C) + S_0 + S_i \tag{23}$$

where C is the concentration of the pollutant, $\mu g/m^3$, at any instant $t(s)$. The second term on the left-hand side represents advection; $\vec{v}$ (m/s) is the mean wind velocity (with horizontal and vertical components) and S_0, S_i ($\mu m^3/s$) are the pollutant source and sink terms, respectively (Piedelievre et al., 1990).

To simplify the diffusion term, turbulent diffusion was modelled using only dominant diagonal terms of the turbulent diffusivity tensor. The turbulent diffusion term $K(x, t)$ is written using the gradient transport theory, or the K-theory (Smagorinsky et al., 1965). The turbulent fluxes are assumed to be proportional to local mean concentration gradients as:

$$\nabla(K \nabla C) = \frac{\partial}{\partial x} K_x \frac{\partial C}{\partial x} + \frac{\partial}{\partial y} K_y \frac{\partial C}{\partial y} + \frac{\partial}{\partial z} K_z \frac{\partial C}{\partial z} \tag{24}$$

3.2.2 Source term

The source uses an isotropic Gaussian distribution, which depends only on distance d from the source (Zannetti, 1990):

$$S_0(d) = \frac{\partial C}{\partial t}(d) = \frac{Q(t)}{2\pi\sigma_n^2 H} \exp \frac{(-d^2)}{2\sigma_n^2} \tag{25}$$

where $Q(t)$ is the emission term ($\mu g/h$), H is the vertical extension of the pollutant cloud (m) and σ^2_n is the horizontal area of the grid box including the source.

3.2.3 Depositions and chemical transformations

Wet deposition is the washing of the hydrogen sulphide out of the air through precipitation. The rate of wet deposition depends on precipitation intensity and duration. Wet deposition due to scavenging is linearly dependent on the rate of precipitation (Hanna et al., 1980):

$$S_w = -\frac{EP_r C}{\rho_w h_p} = -K_w C \tag{26}$$

where E is the scavenging ratio, P_r is the rate of precipitation (in kg/m^{2}s), ρ_w is the specific mass of water, h_p is the thickness of the precipitation layer (constant at 2000 m), C is the concentration of hydrogen sulphide in the precipitation layer and K_w is the wet deposition coefficient.

Dry deposition, S_d, describes the uptake of hydrogen sulphide at the earth's surface by soil, water or vegetation. The dry deposition is taken as from the layer closest to the earth's surface. It is a uniform and continuous process, slower than wet deposition and it can take several days to eliminate most of the pollutant from the atmosphere (Piedelievre et al., 1990):

$$S_d = \frac{-v_d C}{\Delta z} = -K_d C \tag{27}$$

where v_d is the dry deposition velocity, $\Delta z(m)$ is the depth of the layer closest to the ground, C is the concentration of hydrogen sulphide in that layer and K_d is the dry deposition coefficient.

Some hydrogen sulphide is apparently oxidized to sulphur dioxide. In the model, the assumption is that all chemical reactions are proportional to the amount of pollutant. A constant transformation coefficient is chosen for similar weather conditions (Hanna et al., 1980):

$$\frac{\partial C}{\partial t} = -K_t C \tag{28}$$

where K_t is the chemical transformation coefficient. The integral sink can roughly be described by:

$$S_i = -K_w C - K_d C - K_t C \tag{29}$$

3.2.4 Advective term

Wind speed and direction are measured from the nearest meteorological stations. The wind-speed profile based on Cenedese et al., (1997) is used. Logarithmic wind profile is:

$$\frac{u}{u_*}\frac{1}{k}\ln\left(\frac{z}{z_0}\right) \tag{30}$$

For non-zero surface heat flux, Monin-Obukhov length scale L is a measure for the buoyancy influence, because this parameter is the only length scale containing the surface heat flux. The Monin-Obukhov length scale L is defined by (Cenedese et al., 1997) as:

$$L = -\frac{u_*^3 c_p \rho \theta_v}{kgH} \tag{31}$$

where g is the acceleration of gravity, c_p is the specific heat of air at constant pressure, ρ is the density of air, H is the sensitive heat flux and θ_v is the ambient temperature representative of the surface layer.

Assuming that $\xi = z/L$ is a non-dimensional height the wind speed profile for both stable and unstable ABL becomes (Panofsky and Dutton, 1984):

$$\frac{kz}{u_*}\frac{\partial u}{\partial z} = \phi_m(\xi) \tag{32}$$

where $\phi_m = (1-16z/L)^{-1/4}$ for unstable ABL

$\phi_m = 1 + 5z/L$ for stable ABL

These formulations are restricted to a height of 200 m, above which, the wind-speed is assumed to be constant. Wind direction averages, are calculated for one, three and six hour periods during which the wind direction is assumed constant.

3.2.5 Diffusive term

Turbulent diffusion was modelled using only the dominant diagonal terms of the turbulent diffusivity tensor. In so doing, both the horizontal diffusion coefficients are assumed to be equal. They depend on

the stability of the atmosphere via Richardson, based on a stability ratio as discussed by Yates et al. (1974) as:

$$K_x = K_y = K_0 \frac{1-2R_i}{1-R_i} \qquad \text{for } R_i > 0 \tag{33}$$

$$K_x = K_y = K_0 R_{ic} \frac{1+R_i}{R_{ic}+R_i} \qquad \text{for } R_i < 0 \tag{34}$$

where K_0 is the dispersion coefficient, R_i is the Richardson number and R_{ic} is the critical Richardson number.

The vertical diffusion coefficient was estimated using the closure approach (Louis, 1979):

$$K_z = L^2 \frac{\partial v_h}{\partial z} F(R_i) \tag{35}$$

where L is the mixing length, v_h is the horizontal wind and $F(R_i)$ is a semi-empirical function of the Richardson number.

$$L = \frac{kz}{(1+\frac{kz}{150})} \tag{36}$$

where k is the von Karman constant (=0.4).

3.2.6 Plume rise calculations

The height of a rising buoyant plume is a function of wind speed, Richardson number and a buoyancy parameter. The Richardson number is expressed as (Louis et al., 1981):

$$R_i = \frac{g}{\theta}\frac{\partial \bar{\theta}}{\partial z}\left[\frac{\partial |\bar{v}_h|}{\partial z}\right]^2 \tag{37}$$

where θ is potential temperature, g is the gravity acceleration, and $\bar{v}_h$ is the horizontal wind.

The buoyancy parameter (Briggs, 1971) is given by:

$$F = gu\left(D/2\right)^2\left(\frac{T_s - T_\infty}{T_\infty}\right) \tag{38}$$

where T_s is the exit stack gas temperature, T_∞ is the temperature of the ambient air, D is the stack diameter, and U is the stack exit velocity.

The additional height according to Briggs (1971) becomes:

$$\Delta H = 150\frac{F}{u^3} \tag{39}$$

3.2.7 Concentration calculations

The governing equation was solved using an integral finite difference approach, which is flexible because volume can be varied for different blocks. The method is simpler conceptually and

mathematically, and is easier to program for a computer. The equation was integrated with respect to volume as shown next:

$$\iiint \frac{\partial C}{\partial t} dV = \iiint K\nabla(\nabla.C)dV - \iiint \bar{v}(\nabla.C)dV + \iiint S_0 dV + \iiint S_i dV \tag{40}$$

Using the Gauss divergence theorem the equation becomes:

$$V\frac{\partial C}{\partial t} = K\iint \nabla(C.n)ds - \bar{v}\iint (C.n)ds + S_0 V + S_i V \tag{41}$$

Additionally, the equation can be expressed as:

$$V\frac{\partial C}{\partial t} = K\sum(\nabla.C)ds - \bar{v}\sum Cds + S_0 V + S_i V \tag{42}$$

where the integral sign has been replaced by a summation sign, because summation is done for all the surfaces making a block.

Equation 42 was solved explicitly leaving one unknown variable: the concentration of hydrogen sulphide, which is resolved in the next time-step.

3.2.8 Summary

The numerical model uses the C++ programming language for solving the mass balance equation. The language provides an object oriented infrastructure and was used to divide the geothermal field and its environment into a grid consisting of blocks and vertical layers. The size of each block is 250 m by 250 m by 2 m. With such a refined grid, hydrogen sulphide is assumed to have completely filled the block in six minutes, which is the time-step used in the model. After another time-step, an equal amount of hydrogen sulphide is inserted into the model. The plume undergoes significant dilution within the block hosting the source. The location of this block depends on the plume rise. The program then distributes the hydrogen sulphide from the source block to all the blocks and layers depending on the prevailing meteorological conditions. One, three, and six hour averages of wind speed and direction, are calculated and their separate model runs made. The simulated near-ground hydrogen sulphide concentrations are in $\mu g/m^3$.

4. MODELLING RESULTS VERSUS FIELD DATA

4.1 Meteorological data

The models have different meteorological data requirements. AERMET, which is the meteorological pre-processor of AERMOD, requires surface observation and upper-air sounding data. Surface observation data consists of wind speed and direction, dry-bulb temperature, total cloud cover and opaque cloud cover. Upper-air sounding data comprises vertical variations of temperature and altitude. Others include the Bowen ratio, albedo, surface roughness and anemometer height. The meteorological parameters used by the numerical model are extracted from the surface observation data. Thingvellir meteorological station, which is 7 km from the power station, across Lake Thingvallavatn, but at the same elevation as the power station, provided hourly surface observation data, except for total cloud-cover (Figure 2). Cloud-cover measure-ments are only made at Reykjavik meteorological station, which is about 32 km west of Nesjavellir.

Upper-air soundings were obtained from Keflavik Airport, the only location in the country where such measurements are made. The measurements are carried out twice daily, at midday and midnight, using a balloon that is released at 38 m a.s.l. Measurements of temperature and altitude are taken every two seconds. The balloon rises up to between 530 and 550 m a.s.l. Data collection and preparation were performed by the Icelandic Meteorological Office. Figure 2 shows wind speed and direction, rainfall and temperature variation for Thingvellir, and cloud-cover and air pressure variation for Reykjavik meteorological station, which is approximately 30 km west of Nesjavellir.

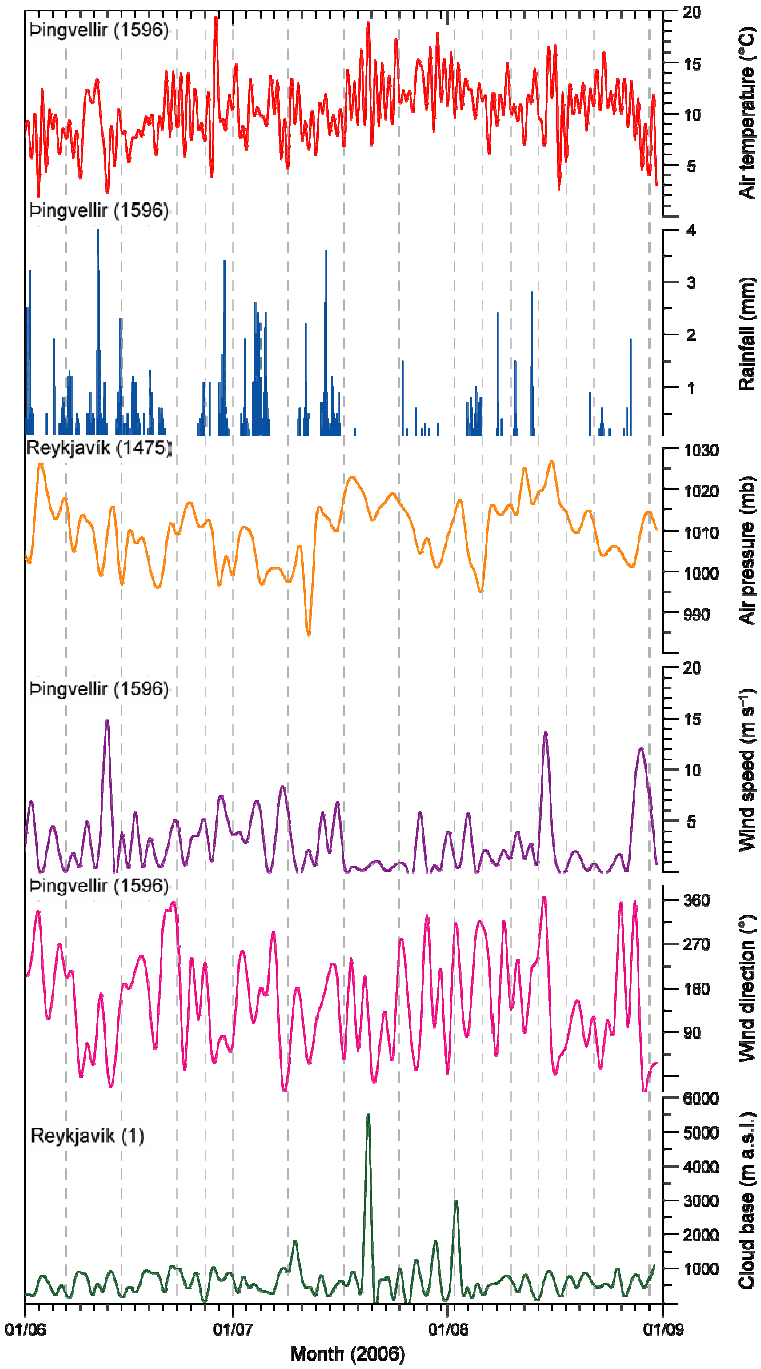

FIGURE 2: Time-series plots of meteorological data from selected weather stations near to Nesjavellir (see Figure 1) between June and August 2006; data provided by the Icelandic Meteorological Office, Reykjavík

4.2 ISC AERMOD View predictions

AERMET, the AERMOD meteorological pre-processor requires three input files. They are: hourly surface observations, upper-air soundings and on-site data, the latter of which is optional. Other parameters are: the Bowen ratio, albedo and surface roughness. Upon processing the input files, AERMET generates two output files which are entered into the AERMOD under the meteorological pathway. AERMOD View, on the other hand, has five input files referred to as pathways. A control pathway specifies the overall job control options such as dispersion options, pollutant and averaging times. A source pathway specifies the source input parameters and source group information such as source types, building downwash and variable emissions. A receptor pathway specifies the receptor locations (modelling area) for a particular run, defines the number and type of receptors, and defines receptor groups and flagpole options. A meteorological pathway, as mentioned earlier, inputs the AERMET output files and specifies the particular days or range of days to process from the sequential meteorological input file. The output pathway, on the other hand, specifies the output options for a particular run such as contour plot files and threshold violation files. Table 1 shows the emission parameters for Nesjavellir power station. Non-condensable gases are either pumped to the cooling tower and released at a high upward velocity below the cooling tower fans or

released through the condensers depending on the prevailing wind direction. Their release was assumed to be through the cooling towers throughout the modelling period.

TABLE 1: Emission parameters for the Nesjavellir geothermal power station

Parameter	Cooling tower 1	Cooling tower 2	Cooling tower 3	Cooling tower 4
Tower height (m)	13	13	13	13
Tower inside diameter at release point (m)	8.9	8.9	8.9	8.9
Gas exit velocity (m/s)	67.2	67.2	67.2	67.2
Gas exit temperature (°C)	33.7	133.7	33.7	33.7
H_2S flowrate (g/s)	175.2	193.4	200.4	197.9

The model was used as described in the preceding sections to calculate 24-hour monthly average concentrations of hydrogen sulphide. One model run used emission inventories for June and the second, July. The third run was for the three months of June, July and August. All the runs used the meteorological fields obtained from the Icelandic Meteorological Office. The model outputs the near-ground concentrations in $\mu g/m^3$. Figure 3 shows the predicted hydrogen concentrations for June. The maximum predicted concentrations occurred some distance away from the power station. Maximum levels of hydrogen sulphide were found to the east and southwest of the power station. Other areas, with high concentrations, were found on the northeast side of the modelling area. Generally, the

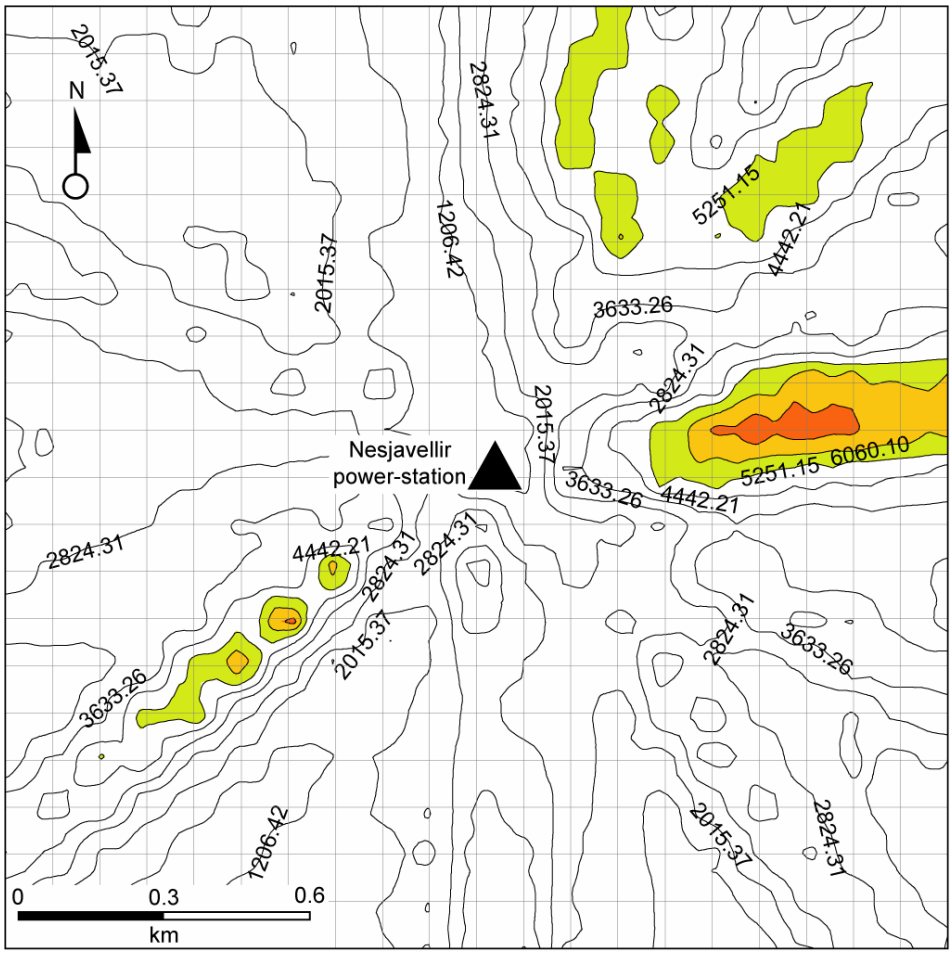

FIGURE 3: Predicted hydrogen sulphide concentrations in June 2006; data are referenced to the ISN93 datum

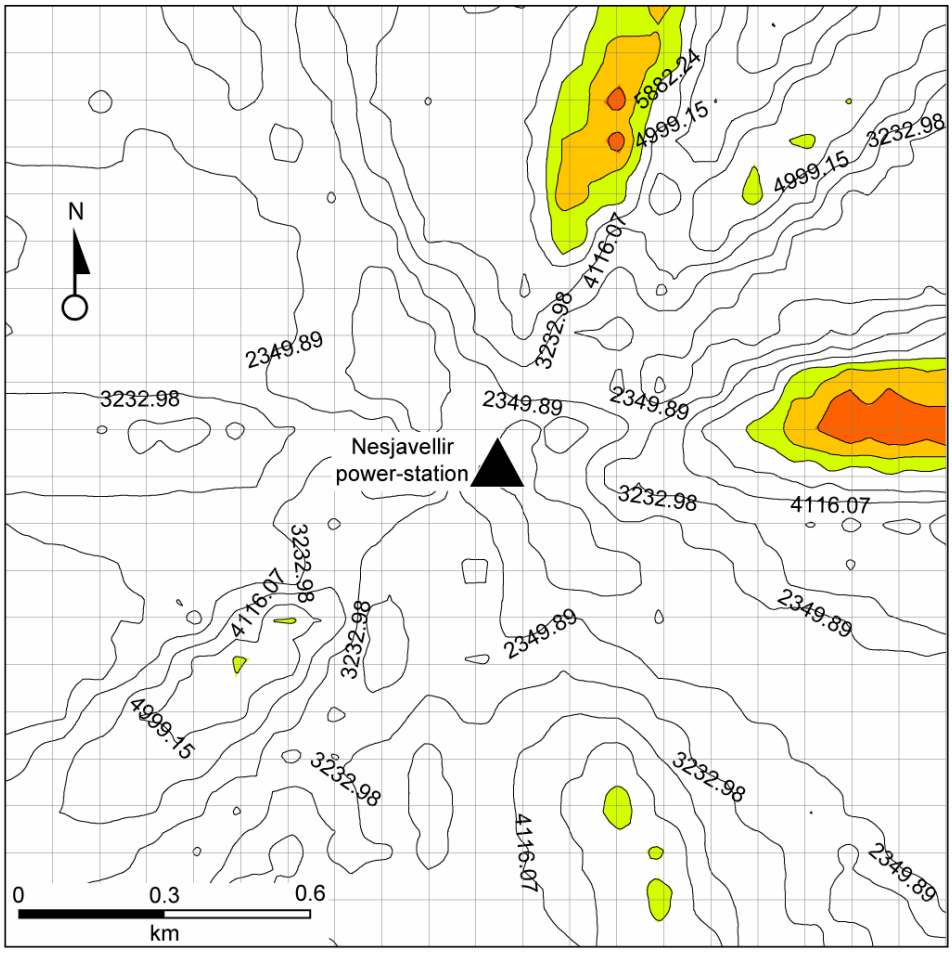

FIGURE 4: Predicted hydrogen sulphide concentrations in July 2006; data are referenced to the ISN93 datum

concentrations increased away from the power station though there were some lower concentrations especially to the south and northwest of the modelling area. The concentrations for June ranged between 0.03 and 5.5 ppm. The concentrations were less than 10 ppm, which is the threshold for workers set by the National Institute for Occupational Safety and Health (NIOSH).

For July, as can be inferred from Figure 4, the overall concentrations within the modelling area increased. Concentrations ranged between 0.4 and 6.1 ppm. This may be attributed to the fact that June (Figure 3) had higher wind speeds than July. Slow winds will cause less mixing of hydrogen sulphide with fresh air resulting in less dilution and hence higher concentrations. Areas with the highest concentrations are found to the east and northeast of the power station. There are pockets with rather high levels of concentrations to the southeast and southwest of the power station.

Figure 5 shows the predictions for the three months (June, July, and August). Note that, high-concentration areas were well-distributed within the modelling area. Areas with concentrations exceeding 3.9 ppm were found to the north, east, and west and at some isolated points to the south. This can be attributed to the variability of wind direction throughout the study period. Maximum concentration levels occurred on the northern and eastern sides of the modelling area. There was an overall increase in concentrations with peaks of 6.4 ppm. However, this is far below the hazardous threshold for humans.

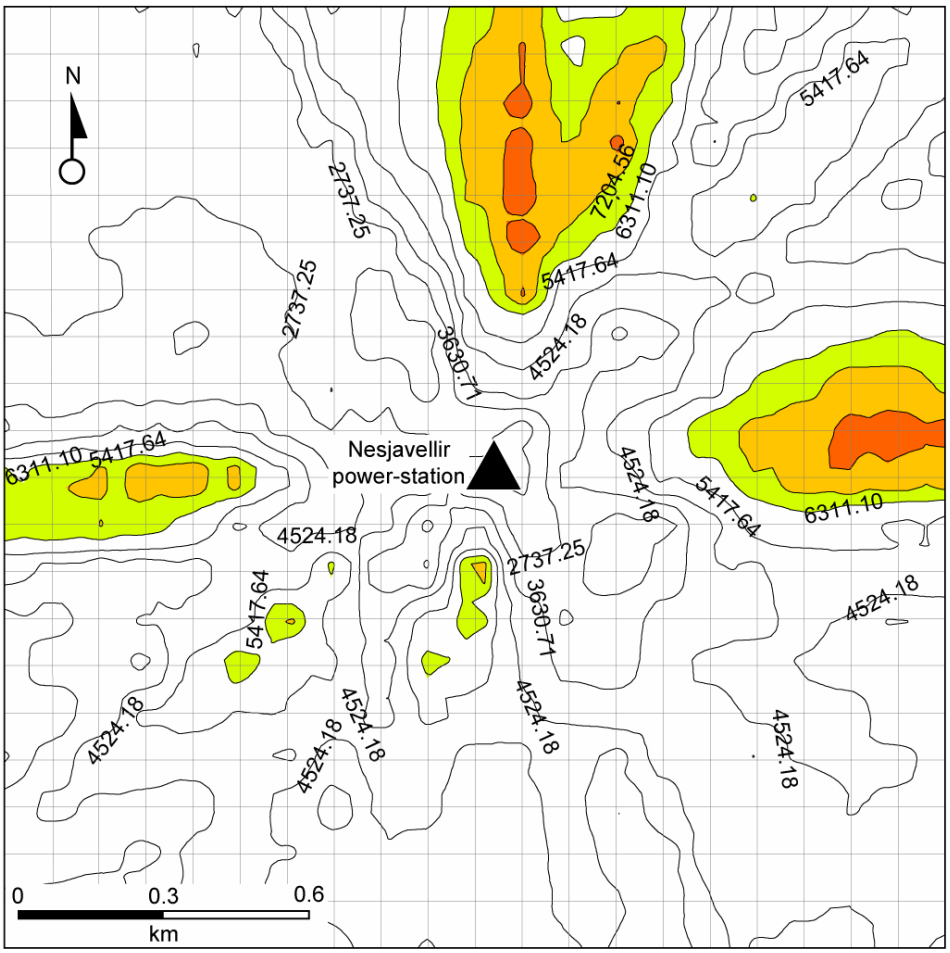

FIGURE 5: Predicted hydrogen sulphide concentrations for June, July, and August 2006; data are referenced to the ISN93 datum

In all three scenarios discussed, the near-ground concentrations increased away from the source. This follows from the fact that, on leaving the cooling tower, the plume has initial momentum, a buoyant force resulting from its initial velocity, and lower density due to high temperature. The plume entrains ambient air as it rises and this reduces the plume's upward momentum. When the temperature of the ambient air and that of the plume are equal, hydrogen sulphide being denser than air will move towards the ground but away from the source. Furthermore, the cooling towers are elevated, hence imparting a similar effect on the plume.

4.3 Numerical model predictions

The model was configured with three vertical layers each with 15×15 grid-points with a horizontal resolution of 250 m. The modelling domain was restricted to an area measuring approximately 10 by 10 km around the power station (see Figure 1). The model calculated the concentration of hydrogen sulphide in the ambient air, based on emission estimates calculated using the emissions from the cooling towers. The model produced four output files: one that shows the distribution of concentrations in all blocks for every time-step, another showing the block positions both in the reservoir and the layer and, in addition, the layer in which the block lies; the third file shows all the ten neighbouring blocks for every block; the last output file shows the size of the modelling domain and the total number of blocks in the area.

Separate model runs were made for the months of June and July, using input parameters averaged for the whole of the modelling period. Figure 6 shows the near-ground concentrations of hydrogen

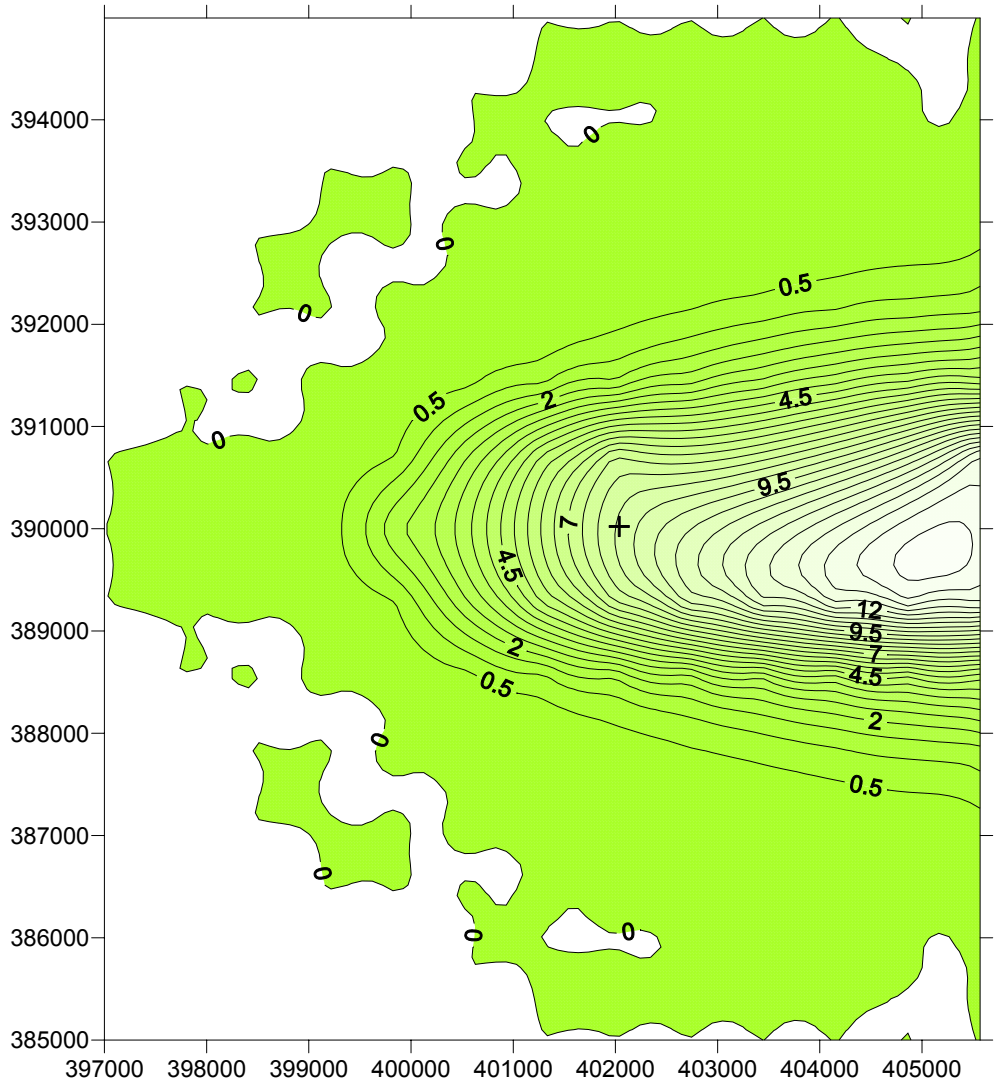

FIGURE 6: Predicted hydrogen sulphide concentrations (ppm) in June 2006; data are referenced to the ISN93 datum

sulphide in ppm for June. Concentrations did not distribute evenly around the power station. The maximum concentration occurred some distance away from the power station. The plume was pushed away by strong winds observed in June (see Figure 2). Figure 7 shows the concentration distribution for July. Concentration variations assumed a similar trend to that observed in June, but the overall concentrations within the modelling domain increased. The point of maximum concentration was nearer to the power station than in the previous case. These results show the effect of wind conditions over plume dispersion; it is possible to establish that stronger winds cause more dilution of hydrogen sulphide due to improved mixing with fresh air.

In order to evaluate the performance of the models, the predicted concentrations were compared with field measurements of near-ground hydrogen sulphide concentrations around the power station. Figure 8 shows the field measurements performed on 12 June 2006. The measured concentrations in the vicinity of the power station indicated high levels of hydrogen sulphide ranging between 10 and 170 ppm. Points of maximum concentration were located due east and south of the power station. These values are high because they are on-the-spot measurements compared to the predicted results, representing 24 hour averages. Shorter time averages were usually higher compared to those averaged for a longer period. However, they followed the same dispersion trends (see Figure 8). In addition, the dispersion models did not take into account background emissions resulting from geothermal manifestations, which would certainly affect the measured concentrations.

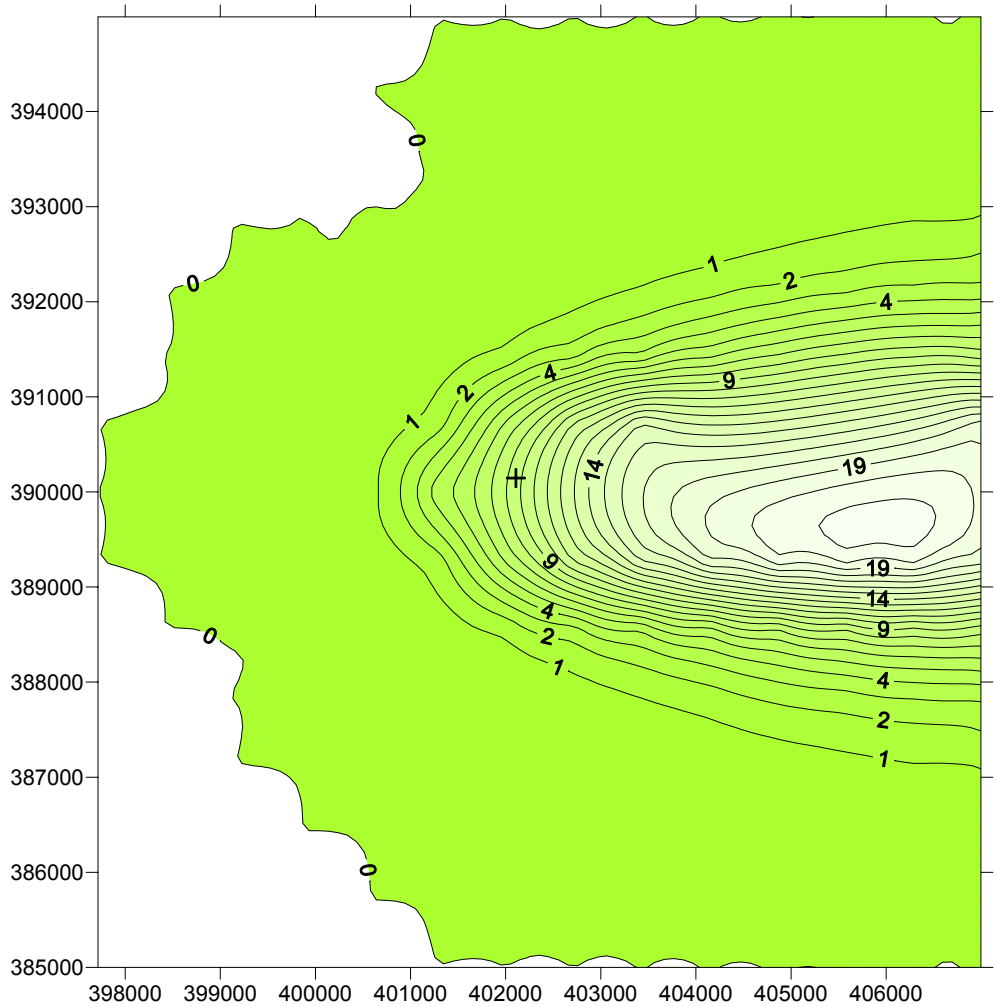

FIGURE 7: Predicted hydrogen sulphide concentrations (ppm) in July 2006; data are referenced to the ISN93 datum

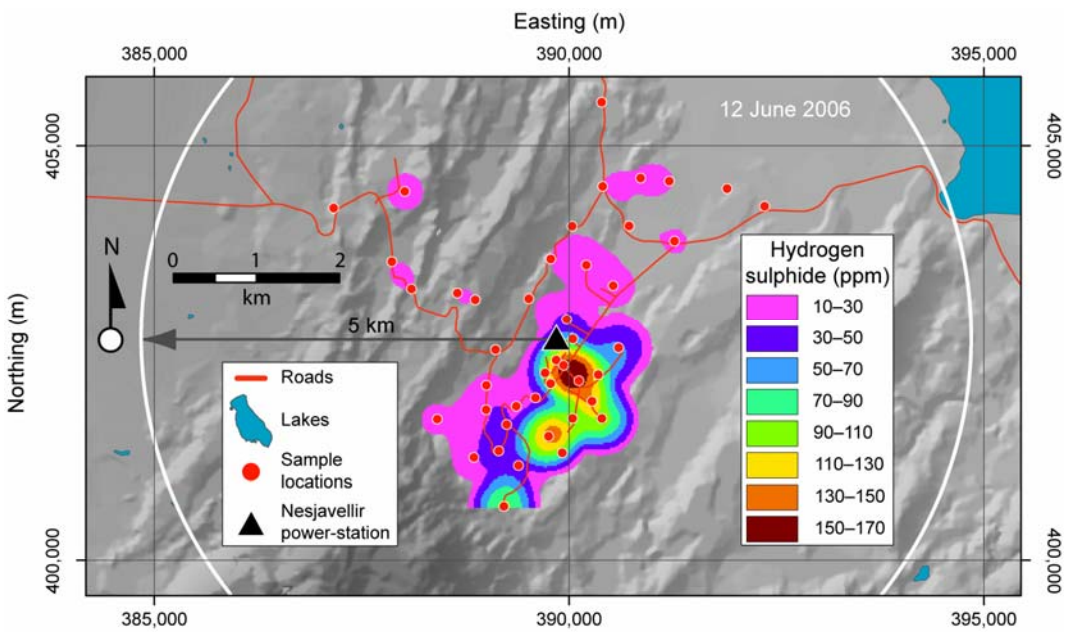

FIGURE 8: Field measurements of hydrogen sulphid concentrations for 12 June 2006; data are referenced to the ISN93 datum

5. ASSESSMENT OF MODELLING RESULTS

AERMOD, a model known for consistency in predicting near-ground concentrations in various situations, showed nearly un-biased levels of concentration throughout the modelling area. Generally, the near-ground concentrations increased away from the source. The adjacent regions, especially to the east, presented relatively high concentration levels, which can be attributed to the prevailing wind direction in the region. However, owing to the ever-changing wind direction in Iceland, the prevailing wind failed to distribute hydrogen sulphide evenly within the modelling field. This can be attributed to local topography. The high terrain characteristic of the Nesjavellir geothermal area drives the wind from southwest and west to northeast and easterly directions, consequently increasing concentrations in the northern and eastern sides of the power station.

The results show that the models demonstrated good capabilities for describing both spatial and temporal characteristics of hydrogen sulphide in the areas surrounding Nesjavellir power station. Despite the meteorological data coming from locations outside the geothermal field, the predictions from both models and the measured values showed significantly similar trends for the near-ground distribution of hydrogen sulphide. Points of high concentrations occurred away from the power station and were distributed in the modelling area. This is because hydrogen sulphide is released from an elevated source, and its temperature is higher than that of ambient air. It will, therefore, rise before descending some distance away from the power station, depending on the direction of the prevailing wind. Though the concentration levels of hydrogen sulphide predicted in most of the areas in the geothermal field were below the threshold levels allowed for humans, they were far above the odour threshold. This implies that the unpleasant smell associated with hydrogen sulphide would be present throughout the modelling area.

Relative to AERMOD, the numerical model overestimated the maximum concentrations to the east of the power station but underestimated the concentrations in all other directions. However, the dispersion trend was similar to that of AERMOD and, to a large extent, replicated the field measurements. As indicated earlier, validation of the numerical model was one of the objectives of this study. Results indicate the model can be adopted for simulating gaseous emissions, albeit with some modifications. The discrepancies on the predicted concentrations were mainly due to the model's inability to accommodate the following factors:

a) Failure to address changes in terrain was the most significant factor. Detailed terrain modelling is important because the wind pattern near the ground surface depends mainly on the frictional resistance of the surface features; hence, meticulous modelling of their influence becomes necessary.
b) b) The average wind speed and direction used by the model was not very representative as there is almost equal wind in all directions with a very slight dominance towards the east. This assumption had a remarkable impact on wind speed and direction and by extension, dispersion of hydrogen sulphide, because the two are the most important meteorological parameters associated with atmospheric dispersion.

6. CONCLUSIONS AND RECOMMENDATIONS

This study modelled the dispersion of hydrogen sulphide emitted from the Nesjavellir geothermal power station using numerical and Gaussian models. The simulated results show that dispersion of hydrogen sulphide is highly weather dependent. The near-ground concentrations are very responsive to variations in wind direction, as observed in the simulations for June, July and August. An increase in overall concentrations for July shows that the dispersion and spatial distribution of hydrogen sulphide mainly depends on wind speed and direction. Increased wind speeds reduce ambient concentration levels of hydrogen sulphide.

The simulation results were lower than the field measurements carried out within the modelling area. The study indicates that both models captured the main features of hydrogen sulphide dispersion. The predictions of the numerical model, though with some discrepancies, provided a good representation of the real-time dispersion in line with the AERMOD model. With some modifications such as the inclusion of changes in terrain and an accommodation of variations in wind speed and direction, the model's predictability would be enhanced.

To improve model predictions, long-term monitoring through field measurements should be done in order to get representative concentrations over greater periods. Permanent sampling points of fixed location should be introduced in the geothermal field so that in conducting simulation studies, the points are given preference as receptor locations.

The numerical model should be adopted as a tool (local model) for conducting comprehensive environmental audits and long-term monitoring of gaseous emissions in Kenya and the rest of the East African region. The importance of a local model is obvious: all the assumptions made in the model development stages are well documented. Lastly, model developers should incorporate the regional meteorological station's method of data collection and storage, thus reducing simulation time and improving modelling efficiency.

ACKNOWLEDGEMENTS

I wish to express my sincere gratitude to Dr. Ingvar B. Fridleifsson, Director of UNU-GTP, for giving me the chance to attend this course. Also, deep thanks to Mr. Lúdvík S. Georgsson, Deputy Director, Mrs. Gudrún Bjarnadóttir, and Ms. Thórhildur Ísberg for their help and kindness during the training period. Special thanks to my supervisor Matthew J. Roberts for his dedicated support and guidance throughout the project writing. I wish to extend my gratitude to Gestur Gíslason of Orkuveita Reykjavíkur and Halldór Ármannsson of Orkustofnun for providing data. To all the UNU Fellows, I am grateful for the company, discussions and sharing we had during the six months we were together.

I am also indebted to Professor Mwakio Tole and Professor John Okumu both of Kenyatta University for their support and the opportunity to attend this training. To my wife Wanja, thanks for your encouragement and unconditional love.

REFERENCES

Briggs, G.A. 1971: Some recent analyses of plume rise observation. In: Englund, H.M., and Beery, W.T. (eds.), *Proceeding of the 2nd International Clean Air Congress*. Academic Press, New York. 1029-1032.

Briggs, G.A., 1973: *Diffusion estimation for small emissions*. Air Resources Atmos. Turb. and Diff. Lab., Environmental Res. Lab., annual report, ATDL-106, 18 pp.

Briggs, G.A., 1984: Plume rise and buoyancy effects. In Haugen, D.A. (ed.), *Atmospheric science and power production.* American Meteorological Society, 327-366.

Brode, R.W., 2006: *AERMOD Technical Forum.* EPA R/S/L Modelers Workshop, San Diego, California, 41 pp.

Brost, R.A., Wyngaard, J.C., and Lenschow, D.H., 1982: Marine stratocumulus layers: Part II: Turbulence budgets. *J. Atmos. Sci., 39*, 818-836.

Cemas, D., and Rakovec, J., 2003: *The impact of emissions from the Sostanj thermal power plant on winter sulphur dioxide pollution in Central Europe.* Environmental Agency of the Republic of Slovenia, Ljubljana, Slovenia, 21 pp.

Cenedese, A., Cosemans, G., Erbrink, H., and Stubi, R., 1997: *Preprocessing of meteorological data for dispersion modelling*. National Environmental Institute Denmark, website: *www2.dmu.dk/atmosphericenvironment/cost/docs.*

Cimorelli, A.J., Perry1, S.G., Venkatram A., Weil, J.C., Paine, R.J., Wilson, R.B., Lee, R.F., Peters, W.D., Brode, R.W., and Paumier, J,O., 2004: *AERMOD: Description of model formulation.* U.S. Environmental Protection Agency report-454/R-03-004, 91 pp.

Garratt, J.R., 1992: *The atmospheric boundary layer.* Cambridge University Press, New York, 334 pp.

Gíslason, G., 2000: Nesjavellir co-generation plant, Iceland. Flow of geothermal steam and non-condensable gases. *Proceedings of the World Geothermal Congress 2000, Kyushu-Tohuku, Japan.* 585-590.

Gissurarson, L.R., and Sigurjónsson, J.A. (eds), 2006: *Environmental report OR 05.* Reykjavik Energy, Reykjavík, report, 40 pp.

Guido S., H.N., 1999: Hydrogen sulphide dispersion model for the Miravalles geothermal field, Costa Rica and groundwater flow and contaminants transport models. Report 4 in: *Geothermal Training in Iceland 1999*. UNU-GTP, Iceland, 97-123.

Gunnarsson, Á., Steingrímsson, B.S., Gunnlaugsson, E., Magnússon, J., and Maack, R., 1992: Nesjavellir geothermal co-generation power plant. *Geothermics, 21-4*, 559-583.

Gunnlaugsson, E., 2003: Environmental monitoring. In: Fridleifsson, I.B., and Gunnarsson, M.V. (eds.), *Lectures on the sustainable use and operating policy for geothermal resources*. UNU-GTP, Iceland, publ. 1, 67-78.

Hanna, S.R., Briggs, G.A., and Hosker, R.P.Jr., 1980: *Handbook on atmospheric diffusion*. Oak Ridge, Tennessee, 743 pp.

Hayward, J.J., 2001: *Summary of toxicity of hydrogen sulphide*: North Carolina Department of Environment and Natural Resources, website *http://daq.state.nc.us/toxics/risk/sab/ra/.*

Hicks, B.B., 1985: Behaviour of turbulent statistics in the convective boundary layer. *J. Appl. Meteor., 24,* 607-614.

Hirsch, A.R., and Zavala, G., 1999: Long-term effects on the olfactory system of exposure to hydrogen sulphide, *Occup. Environ. Med.*, *56*; 284-287.

Kristmannsdóttir, H., and Ármannsson, H., 2003: Environmental aspects of geothermal energy utilization. *Geothermics 32*, 451-461.

Kristmannsdóttir, H., Ármannsson, H. and Árnason, K., 2000: An enforcement project on Environmental Impact of geothermal exploitation in Iceland. *Proceedings of the World Geothermal Congress 2000, Kyushu - Tohoku, Japan*, 633-638.

Kristmannsdóttir, H., Sigurgeirsson, M., Ármannsson, H., and Hjartarson, H., 1997: Emission, dispersion and reaction of H_2S in steam from geothermal fields in Iceland, *Proceedings of NEDO International Geothermal Symposium, Sendai, Japan,* 261-269.

Louis, J.F., 1979: A parametric model of vertical eddy fluxes in the atmosphere. *Bound. Layer Meteor., 17,* 187-202.

Louis, J.F., Tiedtke, M., and Geleyn, J.F., 1981: A short history of the operational PBL parameterisation at ECMWF. *Proceedings of the ECMWF Workshop on PBL Parameterization*, Reading, 59-79.

Marani, M., Tole, M.P., and Ogallo, L.J., 1995: Concentration of H_2S in the air around the Olkaria geothermal field, Kenya. *Discovery and Innovation, 12*, 96 pp.

Moussiopoulos N., Berge B., Bohler, T., de Leeuw, F., Gronskei, K.E., Mylona, S., and Tombrou M., 1997: *Ambient air quality, pollutant dispersion and transport models.* European Environmental Agency, Copenhagen, 58 pp.

Noorollahi, Y., 1999: H_2S and CO_2 dispersion modelling for the Nesjavellir geothermal power plant, S-Iceland and preliminary geothermal environmental impact assessment for the Theistareykir area, NE-Iceland: Report 10 in: *Geothermal Training in Iceland 1999*. UNU-GTP, Iceland, 247-284.

Noorollahi, Y., and Yousefi, H., 2003: Preliminary environmental impact assessment of a geothermal project in Meshkinshahr, NW-Iran. *Proceedings of International Geothermal Conference, IGC2003 Reykjavík,* S12-1-11.

Nyagah, E.M., Tole, M.P., Okumu, J., and Rathore, I.V.S., 2006: *A numerical model for determining the dispersion of hydrogen sulphide plume from Olkaria geothermal power station*. Kenyatta University, MSc thesis, 67 pp.

Oke, T.R., 1978: *Boundary layer climates.* John Wiley and Sons, New York, 372 pp.

Panofsky, H.A., and Dutton, J.A., 1984: *Atmospheric turbulence: models and methods for engineering applications.* John Wiley and Sons, New York, 417 pp.

Panofsky, H.A., Tennekes, H., Lenschow, D.H., and Wyngaard, J.C., 1977: The characteristics of turbulent velocity components in the surface layer under convective conditions. *Bound .layer meteor., 11*, 355-361.

Piedelievre, J.P., Musson-Genon, L., and Bompay, F., 1990: An Eulerian model of atmospheric dispersion: First validation on the Chernobyl release. *Applied Meteorology, 29*, 1205–1220.

Sinclair Knight, ESA Pty Ltd, and RPS International Ltd, 1992: *Environmental assessment for North East Olkaria power development project.* Report prepared for Kenya Power Company Ltd.

Smagorinsky, J., Manabe, S., and Halloway, J.L. Jr., 1965: Numerical results from a 9- level general circulation model of the atmosphere. *Am. Meteorological Society 93,* 727-768.

Tonnesen, G., Olaguer, J., Bergin, M., Russell, T., Hanna, A., Makar, P., Derwent, D., and Wang, Z. 1998: *Air quality models*. NARSTO, website: *www.narsto.org/files/files/.*

Van Ulden, A.P., and Holtslag, A.A.M., 1985: Estimation of atmospheric boundary layer parameters for diffusion applications. *J. Climate Appl. Meteor., 24*, 1196-1207.

Venkatram, A., 1980: Estimating the Monin-Obukhov length in the stable boundary layer for dispersion calculations. *Bound Layer Meteor., 19,* 481-485.

Wiel, J.C., 1988: Dispersion in the convective boundary layer. In: Venkatram, A., and Wyngaard, J.C., (eds.), *Lectures on air pollution modelling.* American Meteorological Society, 167-227.

World Bank, 1998: *Pollution prevention and abatement handbook, Principles of industrial pollution management*. The World Bank Group, 471 pp.

Wyngaard, J.C., 1988: Structure of the PBL. In: Venkatram, A., and Wyngaard, J.C. (eds), *Lectures on air-pollution modelling*. American Meteorological Society, 9-61.

Yates, W.E., Akesson, N.B., and Cowden, R.E., 1974: Criteria for minimizing drift residues on crops downwind from aerial applications. *Transactions ASAE, 17-4,* 637-632.

Zannetti, P., 1990: *Air pollution modelling theories, Computational methods and available software.* Van Nostrand Reynolds, New York, USA, 456 pp.